Thermochimica Acta, 202 (1992) 1–16
Elsevier Science Publishers B.V., Amsterdam

Kinetic analysis of thermal decomposition reactions. Part VI. Thermal decomposition of manganese(II) acetate tetrahydrate

El-Husseiny M. Diefallah
Faculty of Science, Benha University, Benha (Egypt)

(Received 27 September 1991)

Abstract

The kinetics of the thermal decomposition of manganese(II) acetate tetrahydrate were studied using isothermal and dynamic thermogravimetric techniques. The dehydration of the tetrahydrate proceeds via a two-stage reaction, each stage involving loss of two water molecules, while the thermal decomposition of the anhydrous salt proceeds in one step to MnO. Kinetic analysis of isothermal data of the three decomposition reactions, when compared with the various solid state reaction models, showed that the reactions are best described by the phase boundary and random nucleation models. Kinetic analysis of the dynamic TG curves were discussed with reference to a composite integral method, in comparison with the integral methods due to Coats and Redfern and to Ozawa. The activation parameters were calculated and the results of the isothermal and dynamic integral methods were compared and discussed.

INTRODUCTION

The theories of the rate processes of heterogeneous reactions have been the subject of various studies. There is considerable diversity of mechanisms by which solids react and there are a variety of factors which may control, determine, influence or modify the rate-limiting processes [1]. The kinetics of the thermal decomposition of solids are affected by experimental factors [2–4], such as heating rate, particle size, sample mass and holder design. Two further important factors are the effect of the enthalpy of reaction upon the sample temperature and the atmosphere. Moreover, the use of different methods of kinetic analysis of both isothermal and non-isothermal thermogravimetric data obtained on one system usually gives different results. Such a large number of complications makes a theoretical analysis of a thermal, heterogeneous decomposition reaction very difficult [4]. In such a reaction, there is an interface between the reacting phases,

Correspondence to: El-H.M. Diefallah, Faculty of Science, Benha University, Benha, Egypt.

and after formation of stable nuclei and their growth above the critical size, some (or all) of the following steps take place: mass transfer to the interface, reaction at the boundary, mass transfer of the products away from the interface or grain boundary movement, and heat transfer to or from the boundary. The slowest of these steps will be the rate-determining step.

Although several studies have been published on the thermal properties of metal acetates [2,5–9], relatively little has been done on the kinetics of decomposition of these compounds. Emphasis has been on the identification of products and of intermediate solid phases appearing during the decomposition process. The thermal decomposition of some Group II metal acetates [5] up to 500°C showed that carbonates were produced in the case of barium and strontium, and oxides in the case of magnesium, cadmium and zinc. In the thermal decomposition of hydrated copper(II) acetate [6], dehydration in vacuo occurs at about 180°C followed at higher temperatures by rapid decomposition to CuO, with water, acetone, and carbon dioxide as the major volatile products. The study of the thermal decomposition of manganese(III) acetate dihydrate in air proceeds in two steps to give $Mn(OH)Ac_2$ at about 130°C and Mn_2O_3 above about 255°C; whereas in nitrogen, decomposition proceeds in three stages to give $Mn(OH)Ac_2$ at about 70°, followed by the formation of $Mn_2(CO_3)_3$ at about 210°C and then $MnCO_3$ above 260°C [7]. The TG curve of the thermal decomposition of manganese(II) acetate tetrahydrate [2] in a nitrogen atmosphere shows a two-stage decomposition process without points of inflection. The first stage (25–130°C) corresponds to dehydration, whereas the second stage (260–350°C) involves the simultaneous loss of acetone and carbon dioxide and the formation of MnO. In air, however, the water loss may appear to occur in two stages and the loss of acetone and carbon dioxide may be accompanied by oxidation of manganese and formation of Mn_2O_3. The study of the thermal decomposition of magnesium acetate tetrahydrate [8] showed that in open atmosphere and in a completely sealed system, the dehydration is a single-stage loss of water, whereas in the case of a quasi-sealed system, the stable monohydrate was obtained.

In the present study, the kinetics of the thermal decomposition of manganese(II) acetate tetrahydrate were studied using isothermal and dynamic thermogravimetric techniques. Kinetic analysis of data were performed and considered with reference to the various theoretical models; the results of the different methods were compared and discussed.

EXPERIMENTAL

The manganese acetate tetrahydrate samples used were BDH, reagent grade, used without further purification. The starting material was sieved

and samples of particle size less than 117 μm were used for simultaneous DTA–TG experiments using a Shimadzu DT30 thermal analyzer. Samples were placed in aluminum crucibles 0.1 cm^3 in volume which were loosely covered. The sample weight in the Al cell of the thermal analyzer was kept at about 6 mg in all experiments, in order to ensure linear heating rate and accurate temperature measurements. The experiments were performed under isothermal conditions or at different specified heating rates under air or nitrogen at a flow rate of 3.0 l h^{-1}.

RESULTS AND DISCUSSION

Manganese(II) acetate tetrahydrate starts to lose water at temperatures slightly above room temperature to produce the anhydrous salt which then decomposes to MnO at about 320°C. The DTA–TG curves in flowing air and nitrogen are shown in Figs. 1 and 2, and in general the results agree with those reported in the literature [2]. The results show how the peaks in the DTA correspond closely to the weight changes observed on the TG trace. The broad endothermic dehydration clearly shows three minima in air or nitrogen at about 70, 90 and 120°C. In some experiments the last two peaks are overlapping. The TG curve, however, shows that dehydration proceeds in two steps, each involving the loss of two water molecules. The DTA curves reveal that dehydration may involve decomposition in stages: incongruent melting and evaporation of liquid water [2].

The TG curves showed that the decomposition of the anhydrous salt proceeds in one step with the expected loss in weight to MnO and with the simultaneous loss of acetone and carbon dioxide. In nitrogen, the DTA curve showed a dented endothermic peak at about 320°C, which indicates that the main acetate decomposition occurs in at least two stages. The two-stage decomposition of the anhydrous salt may indicate at least partially, as in the case of cadmium acetate [5], the presence of an intermediate mixed acetate–oxide salt. In air, however, decomposition of the acetone vapor occurs on contact with the oxygen, with the consequent marked exothermal activity. The endothermal decomposition is overshadowed by the exothermal reaction giving two well-defined steps in the DTA and with peak temperatures at about 300 and 320°C.

The results of TG measurements showed a two-stage loss of water, both under nitrogen and air, consistent with the loss of two moles of water during each stage. The two stages were resolved in the TG curve shown in Fig. 3 to permit kinetic analysis of the two stages separately. If we denote the fractional decomposition at the end of the first stage α°_1, then the fraction of salt decomposed in this first stage is $\alpha_1 = (\alpha/\alpha^\circ_1)$, where α is the total fractional decomposition and $\alpha < \alpha^\circ_1$ for the first stage. The fraction reacted in the second dehydration step α_2 is given by $\alpha_2 = (\alpha - \alpha^\circ_1/\alpha^\circ_2 - \alpha^\circ_1)$ where α is the total fractional decomposition and α°_2 is the

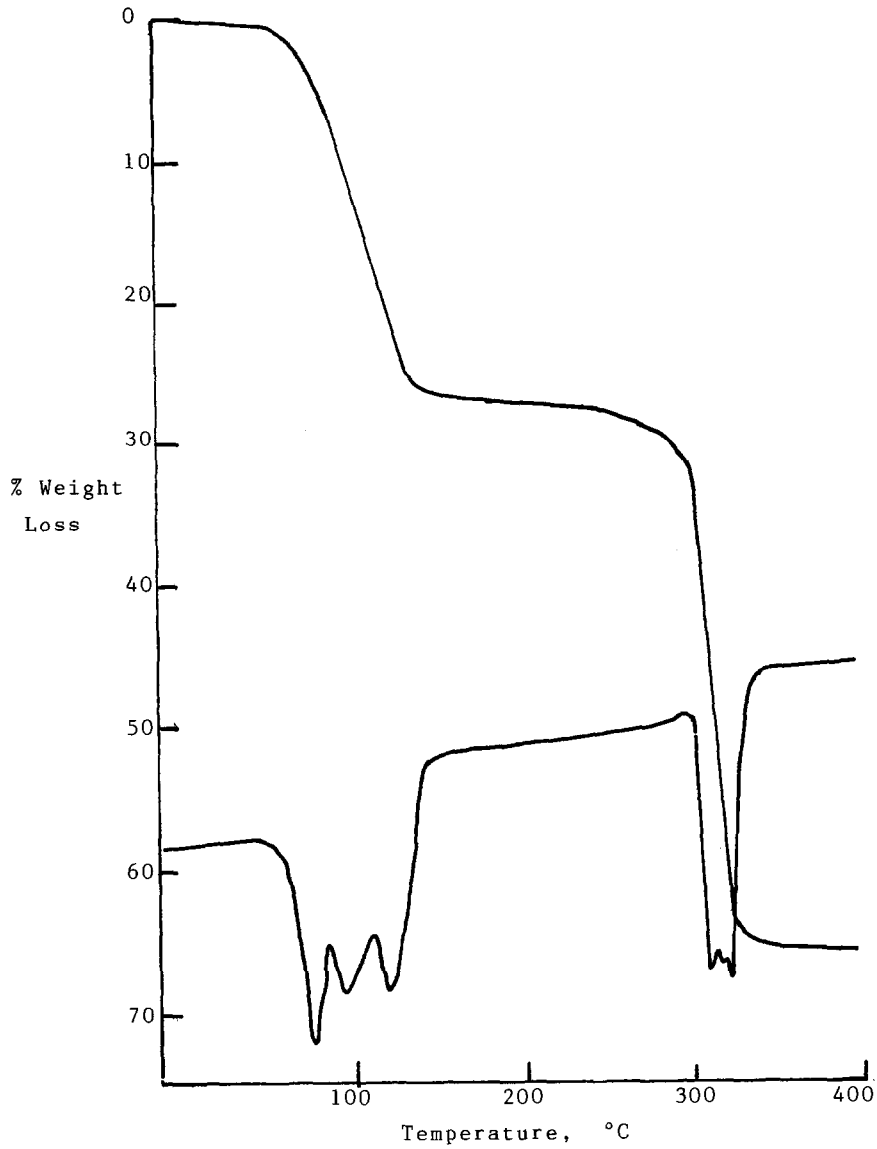

Fig. 1. DTA–TG curves of manganese(II) acetate tetrahydrate in nitrogen. Heating rate = 15°C min^{-1}.

fractional decomposition at the end of the second stage. The third stage corresponds to the main decomposition of the anhydrous salt to MnO in the temperature range 260–350°C and the isothermal fractional reaction–time curves are shown in Fig. 4.

The kinetic analysis of the two dehydration steps and of the decomposition of the anhydrous manganous acetate were performed with reference to the different models of heterogeneous solid-state reactions [10–14]. Under

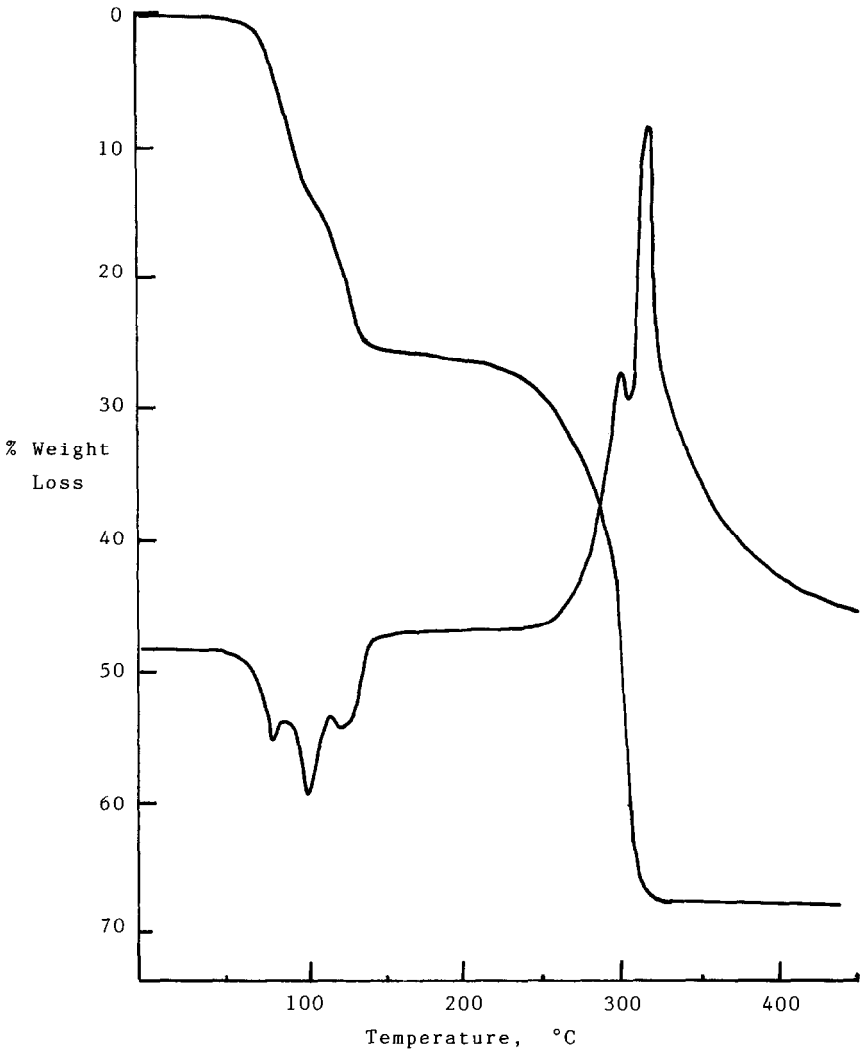

Fig. 2. DTA–TG curves of manganese(II) acetate tetrahydrate in air. Heating rate = 15°C min^{-1}.

isothermal conditions, the fractional reaction–time (α–t) curves are expressed in the form $g(\alpha) = kt$, where k is the rate constant and the function $g(\alpha)$ depends on the mechanism controlling the reaction and on the size and shape of the reacting particles. For the phase boundary controlled reactions, we have the contracting area or R_2 model, $g(\alpha) = 1 - (1-\alpha)^{1/2}$ and the contracting sphere or R_3 model, $g(\alpha) = 1 - (1-\alpha)^{1/3}$. For the diffusion controlled reactions, analyses were performed with reference to a one-dimensional diffusion process governed by a parabolic law, D_1 function, $g(\alpha) = \alpha^2$; a two-dimensional diffusion-controlled process in a cylinder, D_2 function, $g(\alpha) = (1-\alpha)\ln(1-\alpha) + \alpha$; Jander's equation for a

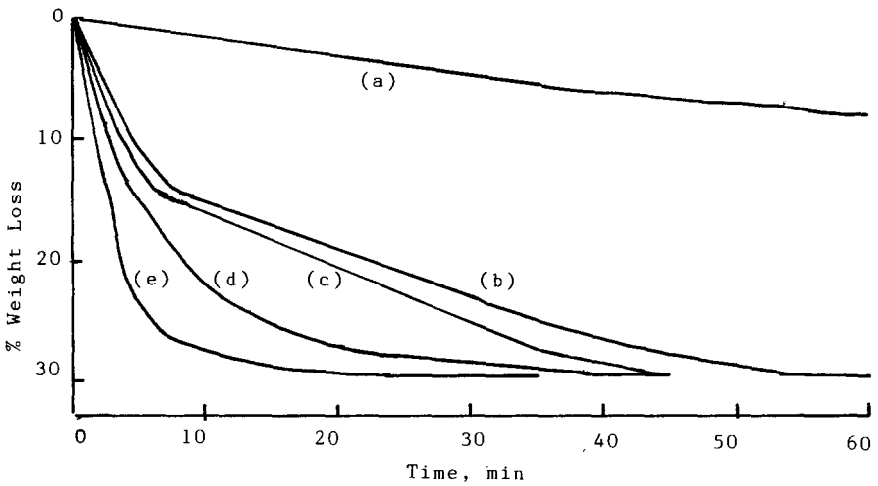

Fig. 3. Isothermal α/t curves for dehydration of manganese(II) acetate tetrahydrate: curve a, 34°C; curve b, 63°C; curve c, 65°C; curve d, 80°C; curve e, 90°C.

diffusion-controlled reaction in a sphere, D_3 function, $g(\alpha) = [1 - (1 - \alpha)^{1/3}]^2$; the Ginsling–Brounshtein equation for a diffusion-controlled reaction starting on the exterior of a spherical particle, D_4 function, $g(\alpha) = (1 - 2\alpha/3) - (1 - \alpha)^{2/3}$; the Zhuravlev–Losokhim–Tempel'man diffusion equation, D_5 function, $g(\alpha) = [1/(1 - \alpha)^{1/3} - 1]^2$; and the Kröger–Ziegler diffusion equation, D_6 function, $k \ln t = [1 - (1 - \alpha)^{1/3}]^2$. If the solid-state reaction is controlled by nucleation followed by growth, then in this case we may have: the Mampel unimolecular law, where the rate-determining step is the nucleation process described by the F_1 function, $g(\alpha) = -\ln(1 - \alpha)$; the Avrami equation for initial random nucleation followed by overlapping growth in two-dimensions, A_2 function, $g(\alpha) = [-\ln(1 - \alpha)]^{1/2}$; the Erofeev equation for initial random nucleation followed by overlapping growth in three dimensions, A_3 function, $g(\alpha) = [-\ln(1 - \alpha)]^{1/3}$; and the Prout–Thomkins equation for branching nuclei, A_1 function, $g(\alpha) = \ln[\alpha/(1 - \alpha)]$.

The results of the kinetic analysis of the isothermal data of the two-stage dehydration reaction and the decomposition of the anhydrous salt, showed that these reactions are best described by phase boundary and random nucleation models. Other models gave a less satisfactory fit to the experimental data. Table 1 shows the activation energies and frequency factors of the three stages of decomposition calculated according to the Arrhenius equation by linear regression (LR) analysis using k values of R_2 and R_3 functions. The results show that the first stage is about 5–6 times faster than the second stage. There is a lowering in activation energy of about 30 kJ mol^{-1} in the second dehydration stage relative to the first stage. However, the decrease in frequency factor is more than enough to compensate for the increase in rate resulting from lowering the activation energy.

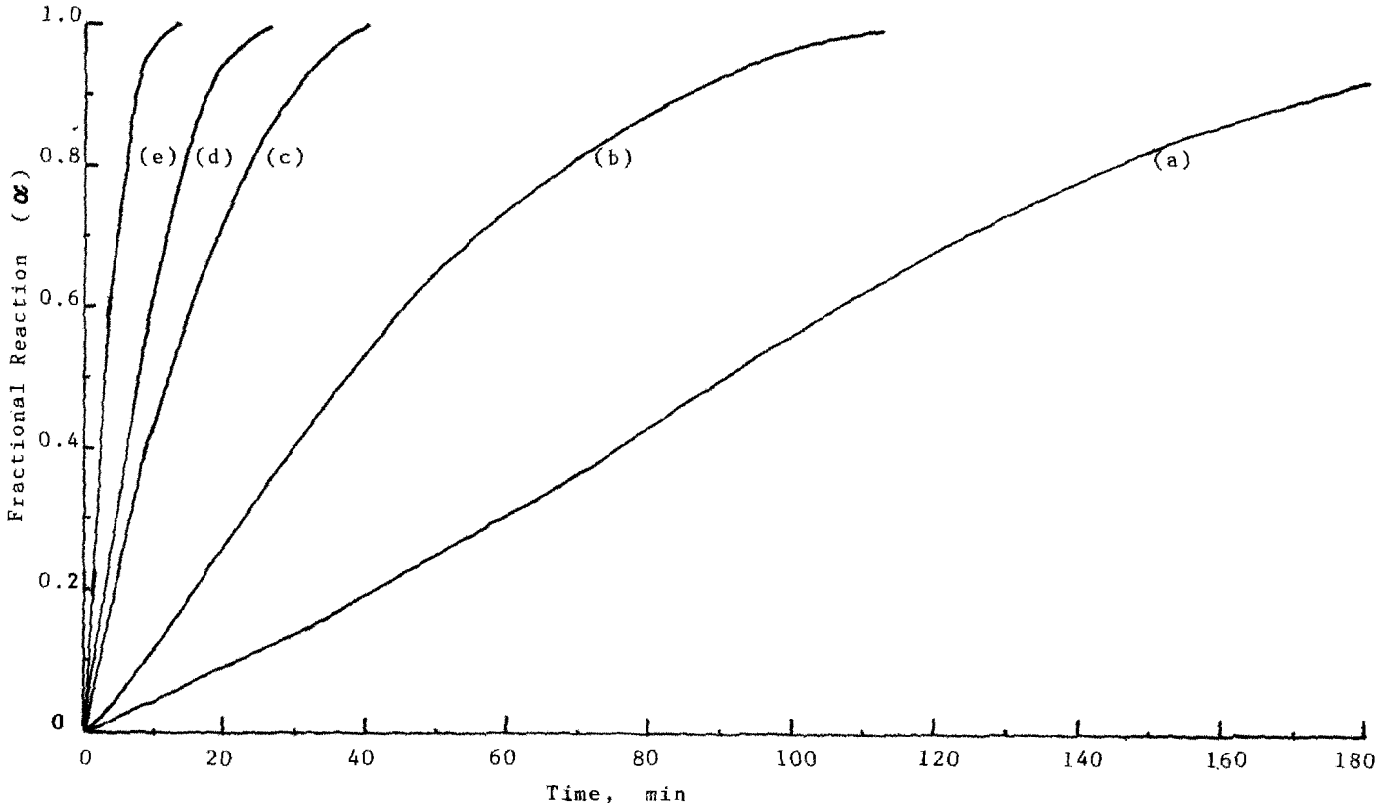

Fig. 4. Isothermal α / t curves for decomposition of manganese(II) acetate: curve a, 266°C; curve b, 279.5°C; curve c, 298; curve d, 307; curve e 316°C.

TABLE 1

Results of the isothermal kinetic experiments on the decomposition of manganese(II) acetate tetrahydrate in nitrogen assuming the contracting area (R_2) and contracting volume (R_3) models

Decomposition Stage	R_2 model		R_3 model	
	E (kJ mol^{-1})	log A (min^{-1})	E (kJ mol^{-1})	log A (min^{-1})
I	99± 4	14.4±0.6	87± 3	12.4±0.4
II	60± 8	3.9±0.5	63± 9	4.1±0.5
III	159±13	13 ±1	161±13	13 ±1

The water in crystalline hydrates may be considered either as crystal water or as co-ordinated water. The strength of binding of these molecules in the crystal lattice is different and, hence, results in different dehydration temperatures and kinetic parameters. The water eliminated at 150°C and below can be considered as crystal water, whereas water eliminated at 200°C and above indicates its coordination by the metal atom. Water molecules eliminated at intermediate temperatures can be coordinatively linked water as well as crystal water. Nikolaev et al. [15] determined the activation energy of dehydration of differently bound water molecules in carbonate chelates of magnesium, calcium and lanthanum. The activation energies for losing crystal water lie in the range 60–80 kJ mol^{-1}, while the values for coordinately bounded water are within the range 130–160 kJ mol^{-1}. The energies of activation and the dehydration temperatures found here for the two dehydration stages of Mn(II) acetate tetrahydrate suggest that the water molecules are present in the crystal as lattice molecules but that the two groups are in different lattice positions.

The kinetics of the main decomposition reaction of the anhydrous salt (stage III) were also investigated under constant heating rate conditions. Figure 5 shows the results obtained from dynamic measurements for samples studied in nitrogen at different heating rates of 1, 2, 5, 10, 15, 20 and 30°C min^{-1}. Because of the conclusions reached from the isothermal studies above, only phase boundary and random nucleation models were used to analyze the results. In the analysis of dynamic TG curves, we assumed the R_2 function and compared three integral methods: the Ozawa [16] method, the Coats–Redfern method [17] and a composite method based either on Doyle's equation [18] (composite method I) or on the modified Coats–Redfern equation [19] (composite method II).

With dynamic techniques the temperature rate is set to a constant value β and the function $g(\alpha)$ is given by Doyle's equation

$$g(\alpha) = (A/\beta)\int_0^T \exp(-E/RT)\,\mathrm{d}T = \frac{AE}{R\beta}P(x)$$

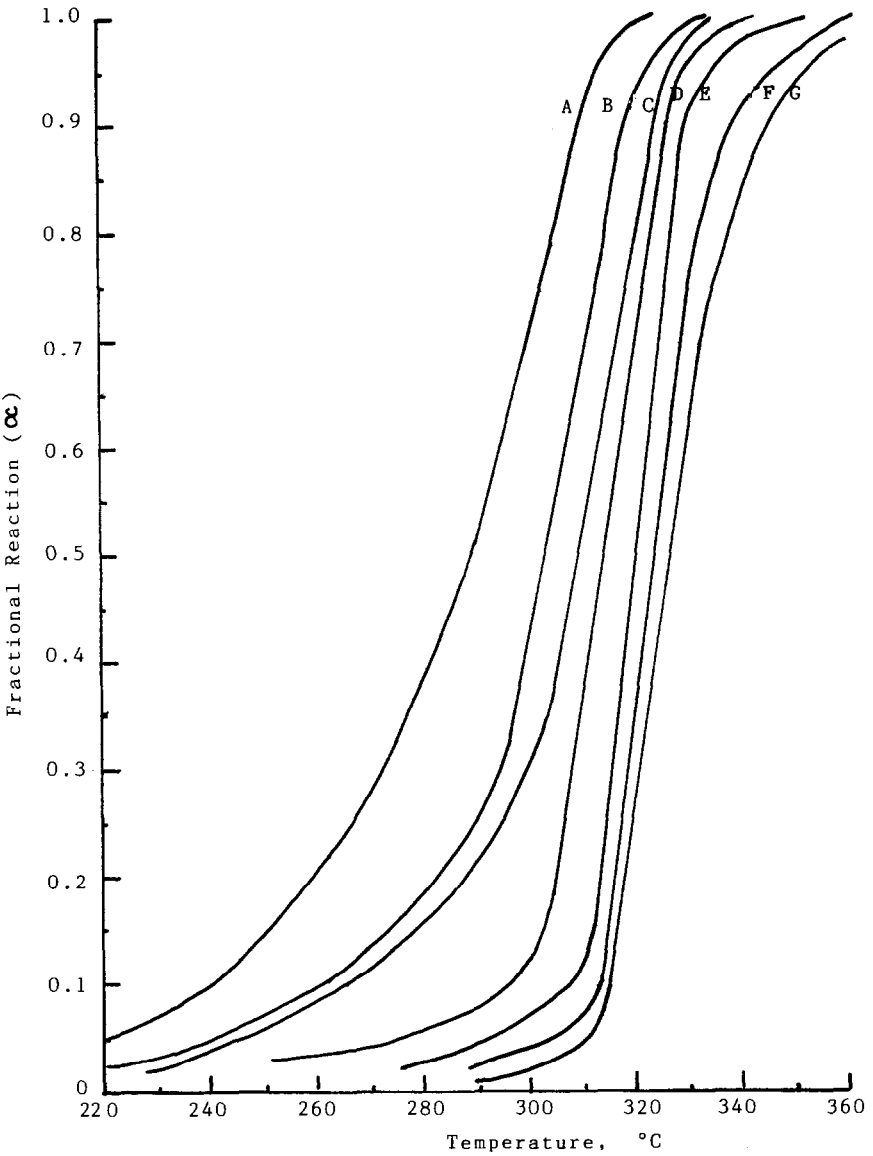

Fig. 5. Dynamic measurements for manganese(II) acetate thermal decomposition. Heating rate: curve A, 1°C min^{-1}; curve B, 2°C min^{-1}; curve C 5°C min^{-1}; curve D 10°C min^{-1}; curve E 15°C min^{-1}; curve F, 20°C min^{-1}; curve G 30°C min^{-1}.

The function $P(x)$ has been defined as

$$P(x) = \frac{e^{-x}}{x} - \int_x^\infty \frac{e^{-u}\,du}{u}$$

where $u = E/RT$ and x is the corresponding value of u at which a fraction

TABLE 2

Results of the dynamic kinetic experiments on the decomposition of anhydrous manganese(II) acetate in nitrogen assuming the contracting area equation

	E (kJ mol^{-1})	log A (min^{-1})
Coats–Redfern method		
$\beta =$ 1°C min^{-1}	79 ± 2	5.4 ± 0.1
2	91 ± 4	6.6 ± 0.3
5	91 ± 5	6.9 ± 0.4
10	167 ± 16	14.0 ± 1
15	205 ± 21	17.4 ± 1.8
21	200 ± 24	16.8 ± 2
30	223 ± 28	19.0 ± 2.4
Average	151 ± 62	12.3 ± 5.8
Ozawa method		
$\alpha = 0.05$	80 ± 7	5.7 ± 0.5
0.10	100 ± 10	7.6 ± 0.8
0.20	145 ± 15	11.8 ± 1.2
0.30	185 ± 22	15.7 ± 1.9
0.40	219 ± 22	20.1 ± 2.0
0.50	252 ± 24	21.9 ± 2.1
0.60	283 ± 24	24.7 ± 2.1
0.70	312 ± 24	27.2 ± 2.1
0.80	316 ± 24	27.5 ± 2.1
0.90	269 ± 32	23.3 ± 2.8
0.95	233 ± 33	20.0 ± 2.8
Average	218 ± 81	18.7 ± 7.1
Composite method I	119 ± 5	9.6 ± 3
Composite method II	114 ± 5	9.0 ± 3

α of material has decomposed. In the Coats–Redfern method [17], the function $g(\alpha)$ is approximated to the form

$$g(\alpha) = \frac{ART^2}{\beta E}\left[1 - \frac{2RT}{E}\right] e^{-E/RT}$$

where α is the fraction of sample decomposed at time t and β is the heating rate. The equation has been written in the form

$$-\ln[g(\alpha)/T^2] = -\ln\frac{AR}{\beta E}\left(1 - \frac{2RT}{E}\right) + \frac{E}{RT}$$

The quantity $\ln[AR/\beta E(1 - 2RT/E)]$ appears to be reasonably constant for most values of E and in the temperature range over which most reactions occur. Table 2 lists the results of calculating E according to the above equation using for $g(\alpha)$ the phase boundary, R_2, equation. Figure 6 shows the graphical representation of the dynamic TG data according to this method. The calculated experimental points showed considerable

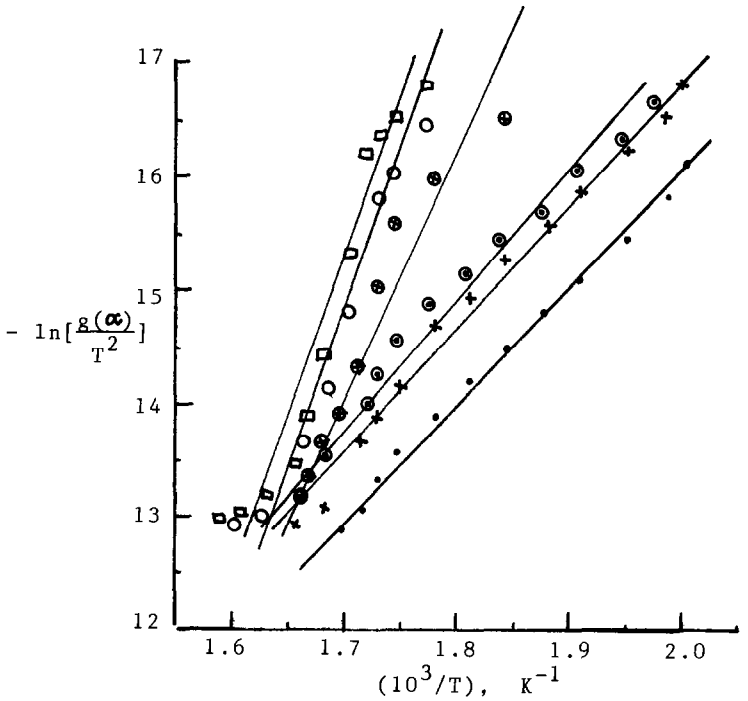

Fig. 6. Coats–Redfern method of analysis. Heating rate: ·, 1°C min^{-1}; ×, 2°C min^{-1}; •, 5°C min^{-1}; ⊗, 10°C min^{-1}; ○, 15°C min^{-1}; □, 20°C min^{-1}.

deviation from a straight line plot especially at the higher heating rates. The statistics of the results greatly improve when only fractions of completed reaction ranging between 0.2 and 0.8 are considered. However, we have tried in the present analysis to include the complete range of α values available and to make comparison between the different methods under these same conditions.

In the Ozawa approximate integral method [16], a master curve has been derived from the TG data obtained at different heating rates (β) using Doyle's equation and assuming that $[(AE/R\beta)P(E/RT)]$ is a constant for a given fraction of material decomposed. The function $P(E/RT)$ was approximated by the equation [18]

$$\log P(E/RT) = -2.315 - 0.4567(E/RT)$$

so that

$$-\log \beta = 0.04567(E/RT) + \text{constant}$$

Hence the activation energy may be obtained from the thermogravimetric data obtained at different heating rates. Figure 7 shows Ozawa plots for α

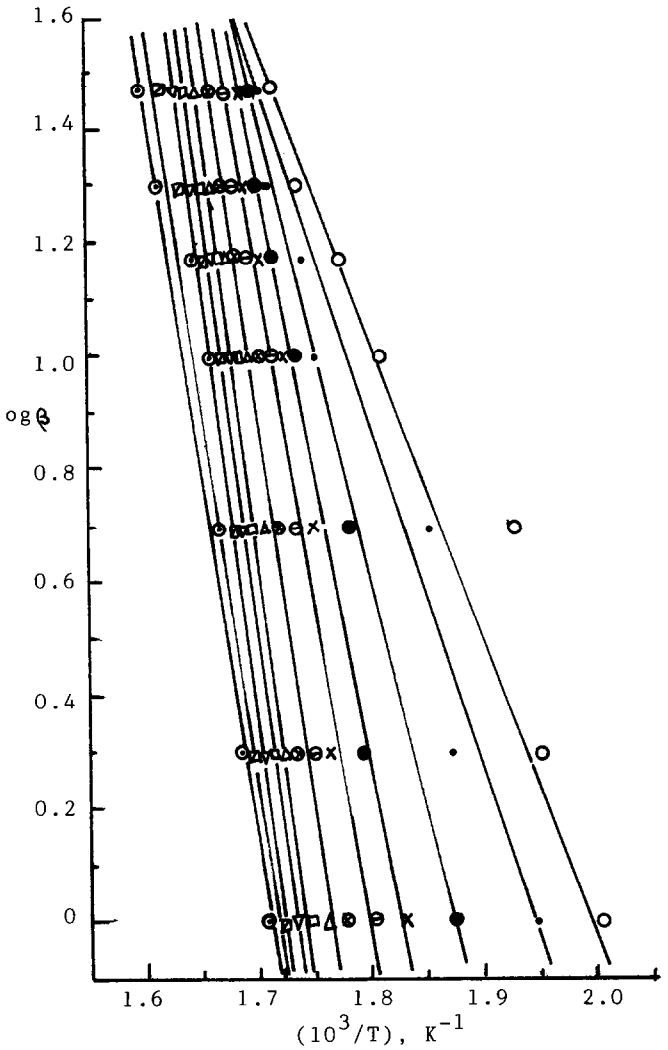

Fig. 7. Ozawa method of analysis. Fractional reaction (α): ○, 0.05; ·, 0.10; ●, 0.20; ×, 0.30; ⊖, 0.40; ⊗, 0.50; △, 0.60; □, 0.70; ▽, 0.80; □, 0.90; ⊙, 0.95.

values ranging between 0.05 and 0.95. The frequency factor was calculated from the equation

$$\log A = \log g(\alpha) - \log\left[\frac{E}{\beta R} P(E/RT)\right]$$

The calculation of E is independent of the reaction model used to describe the reaction, whereas the frequency factor depends on the determined form of $g(\alpha)$. The results of the dynamic TG data analysis according to this method are shown in Table 2. There is a strong dependence of activation

parameters on the α value. The energy of activation and frequency factor first increase with increasing α up to $\alpha = 0.8$, and then decrease. This may indicate the effects of thermal transport and heat of reaction or a change in mechanism during the progress of the reaction.

In the composite methods of analysis of dynamic data, the results obtained not only at different heating rates but also with different α values, are superimposed on one master curve. In the application of composite method (I), use has been made of the modified Coats–Redfern equation [19]

$$\frac{g(\alpha)}{T^2} = \frac{AR}{\beta E} e^{-(E/RT)}$$

The equation was rewritten in the form

$$\ln[\beta g(\alpha)/T^2] = \ln(AR/E) - (E/RT)$$

Therefore, the dependence of $\ln[\beta g(\alpha)T^2]$, calculated for different α values at their respective β values, on $1/T$ must give rise to a single master straight line for the correct form of $g(\alpha)$, and hence a single activation energy and frequency factor can readily be calculated. Figure 8 shows a composite plot according to this method.

The second approach for composite analysis of data depends on Doyle's equation

$$g(\alpha) = \frac{AE}{R\beta} P(E/RT)$$

Again, using the approximation given above for the function $P(E/RT)$, this equation may be rewritten as

$$\log g(\alpha)\beta = \left(\log \frac{AE}{R} - 2.315\right) - \frac{0.4567\,E}{RT}$$

Hence, the plot of the left side of this equation, for the different values of α at their respective β values, versus $1/T$ must give rise to a single master straight line, from the slope and intercept of which single values for both E and $\log A$ may be calculated. Figure 9 shows the results of data analysis performed according to the above equation, again assuming the R_2 model for the reaction interface. Applying LR analysis to the results shown in Figs. 8 and 9 gave the values of the activation parameters shown in Table 2.

The results show that both composite methods of analysis gave equivalent curves and identical values for the activation parameters. This approach involves a complete analysis of all the non-isothermal curves into a single curve. However, Figs. 8 and 9 show that the dependence of $\ln[\beta g(\alpha)]$ or $\ln[\beta g(\alpha)/T^2]$ on the inverse of the absolute temperature is more complex than is suggested by the Arrhenius-type equation and the kinetic

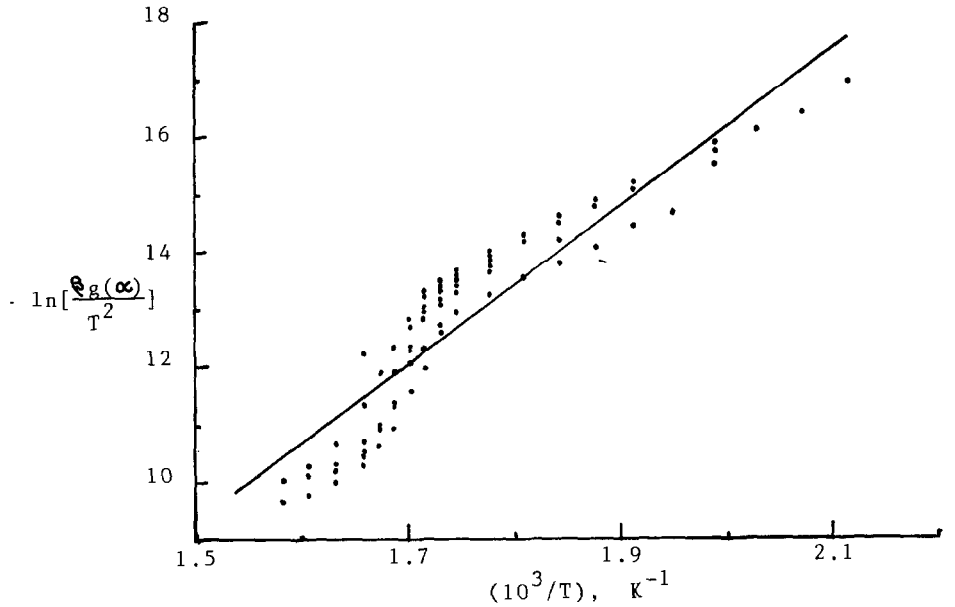

Fig. 8. Composite analysis of dynamic TG data based on the modified Coats–Redfern equation.

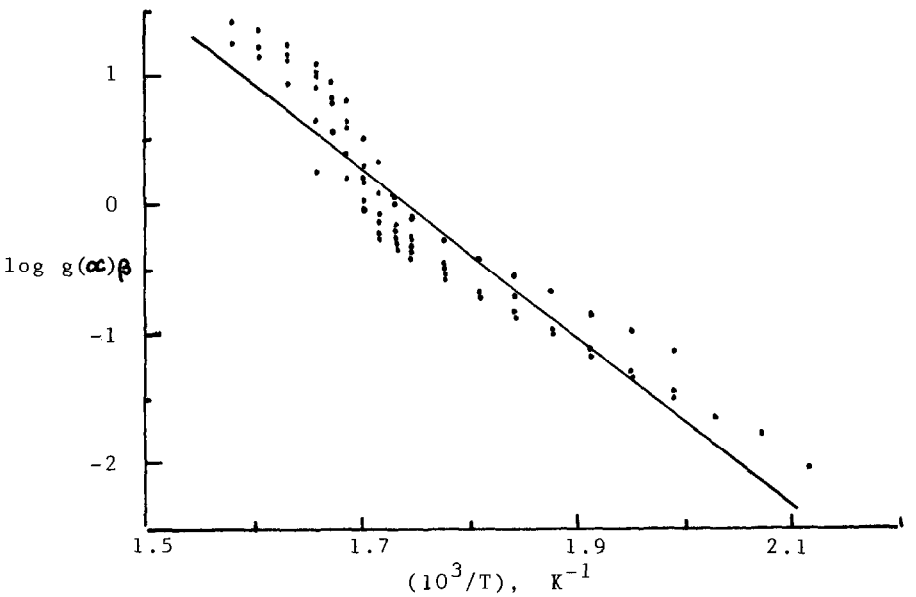

Fig. 9. Composite analysis of dynamic TG data based on Doyle's equation.

model function $g(\alpha)$. The data points showed a break at a temperature of about 315°C ($10^3/T = 1.7$), which indicates that stage III of the main decomposition may take place in at least two steps as has been shown by the DTA curve. This could make the results obtained at the higher temperatures non-isokinetic with the results obtained at the lower temperatures.

The results of data analysis of both isothermal and non-isothermal experiments showed that the kinetic function $g(\alpha)$ is not the factor responsible for the variations in the calculated activation parameters and that the variations are more a function of experimental conditions and the method of data analyses [20]. However, attempts to evaluated activation energies from single non-isothermal experiments, making no assumption about the kinetic form of $g(\alpha)$ appear to give unreliable results [21,22]. The values listed in Table 2 for E and log A calculated by the Coats–Redfern method reflect the well known compensation effect, in which log A increases in line with E as the experimental variables (in this case the heating rate) are changed. That the average value in this case is close to that obtained under isothermal conditions may be entirely fortuitous. Similarly, the values obtained from the Ozawa method simply demonstrate that E and log A vary with α, i.e. that the reaction mechanism varies with the fraction reacted, which itself in these experiments varies with temperature and heating rate. This shows that thermal transport rather than mass transport or chemical process could be the rate determining process for thermal decomposition reactions [23]. The results in the present study illustrate the difficulties of obtaining meaningful kinetic data of a solid state decomposition and suggest that experimental processing parameters which are not included in the kinetic model are important factors which affect the temperature level at different regions of the sample.

REFERENCES

1 V.V. Boldyrev, M. Bulens and B. Delmon, The Control of the Reactivity of Solids, Elsevier, Amsterdam, 1979.
2 A.E. Newkirk, Thermochim. Acta, 2 (1971) 1.
3 P.K. Gallagher and D.W. Johnson, Jr., Thermochim. Acta, 6 (1983) 67.
4 W.W. Wendlandt, Thermal Methods of Analysis, J. Wiley, New York, 1975.
5 H.G. McAdie and J.M. Jervis, Thermochim. Acta, 1 (1970) 19.
6 K.C. Patil, G.V. Chandrashekhar, M.V. George and C.N.R. Rao, Can. J. Chem., 46 (1968) 257.
7 C.P. Prabhakaran and S. Sarasukutty, Thermochim. Acta, 82 (1984) 391.
8 K. Isa and M. Nogawa, Thermochim. Acta, 75 (1984) 197.
9 R. Leibold and F. Huber, J. Therm. Anal., 18 (1980) 493.
10 S.F. Hulbert and J.J. Klawitter, J. Am. Ceram. Soc., 50 (1967) 484.
11 J.H. Sharp, G.W. Brindley and B.N.N. Achar, J. Am. Ceram. Soc., 49 (1966) 379.
12 M.E. Brown, D. Dollimore and A.K. Galwey, Comprehensive Chemical Kinetics, Vol. 22, Elsevier, Amsterdam, 1980.

13 A.M.M. Gadalla, Thermochim. Acta, 74 (1984) 255.
14 M.E. Brown, Introduction to Thermal Analysis, Chapman and Hall, 1988, Chapt. 13.
15 A.V. Nikolaev, V.A. Logvenko and L.I. Myachina, in R.F. Schwenker, Jr., and P.D. Garn (Eds.), Thermal Analysis, Vol. 2, Inorganic Materials and Physical Chemistry, Academic Press, New York, 1969, p. 779.
16 T. Ozawa, Bull. Chem. Soc. Jpn., 38 (1965) 1881; J. Therm. Anal. 2 (1970) 301.
17 A.W. Coats and J.P. Redfern, Nature, 201 (1964) 68.
18 C.D. Doyle, J. Appl. Polym. Sci., 5 (1961) 285.
19 J.M. Criado, Thermochim. Acta, 24 (1978) 186.
20 A.R. Salvador, E.G. Calvo and J.M. Navarro, Thermochim. Acta, 87 (1985) 163.
21 J.M. Criado, F. Rouquerol and J. Rouquerol, Thermochim. Acta, 38 (1980) 2090.
22 D. Dollimore, G.A. Gamlen, J. Rouquerol, F. Rouquerol and M. Reading, Proc. 2nd Eur. Symp. Therm. Anal., ESTA 2, University of Aberdeen, UK, 1–4 Sept. 1981, Heyden, London, 1981, p. 99.
23 P.K. Gallagher and D.W. Johnson, Jr., Thermochim. Acta, 14 (1976) 255.